Journal of Cellular Biochemistry 46:266–276 (1991)

Fluorescent Tetradecanoylphorbol Acetate: A Novel Probe of Phorbol Ester Binding Domains

Margit Balázs, Jánòs Szöllösi, William C. Lee, Richard P. Haugland, Anthony P. Guzikowski, Mack J. Fulwyler, Sandor Damjanovich, Burt G. Feuerstein, and Harrihar A. Pershadsingh

Departments of Laboratory Medicine (M.J.F., B.G.F., H.A.P.), Restorative Dentistry (W.C.L.), and the Brain Tumor Research Center (B.G.F.), University of California, San Francisco, San Francisco, California 94143; Department of Biophysics, University Medical School, Debrecen, H-4012, Hungary (M.B., J.S., S.D.); Molecular Probes Inc., Eugene, Oregon 97402 (R.P.H., A.P.G.)

Abstract Protein kinase C (PKC) has a prominent role in signal transduction of many bioactive substances. We synthesized the fluorescent derivative, phorbol-13-acetate-12-N-methyl-N-4-(N,N'-di(2-hydroxyethyl)amino)-7-nitrobenz-2-oxa-1,3-diazole-aminododecanoate (N-C_{12}-Ac(13)) of 12-O-tetradecanoylphorbol-13-acetate (TPA) to monitor the location of phorbol ester binding sites and evaluate its potential use as a probe of PKC in viable cells. The excitation maximum wavelength of N-C_{12}-Ac(13) is close to 488 nm, facilitating its use in argon-ion laser flow and imaging cytometry. When incubated with 100 nM N-C_{12}-Ac(13) at 25°C, P_3HR-1 Burkitt lymphoma cells accumulated the dye rapidly, reaching maximum fluorescence within 25 min, 20-fold above autofluorescence. Addition of unlabeled TPA significantly decreased the fluorescence of N-C_{12}-Ac(13) stained cells in a dose-dependent manner indicating specific displacement of the bound fluoroprobe. Competitive displacement of [^{3}H]-phorbol-12,13-dibutyrate ([^{3}H]-PBu_2) from rat brain cytosol with N-C_{12}-Ac(13) gave an apparent dissociation constant (K_d) of 11 nM. N-C_{12}-Ac(13) possessed biological activity similar to TPA. Like TPA (final concentration 65 nM) N-C_{12}-Ac(13), at a lower concentration (51 nM), induced expression of Epstein-Barr viral glycoprotein in P_3HR-1 cells, differentiation of promyelocytic HL60 cells, and caused predicted changes in the mitotic cycle of histiocytic DD cells. Microspectrofluorometric images of single cells labeled with N-C_{12}-Ac(13) showed bright fluorescence localized intracellularly and dim fluorescence in the nuclear region, consistent with dye binding mainly to cytoplasmic structures and/or organelles and being mostly excluded from the nucleus. Because of the high level of non-specific binding of N-C_{12}-Ac(13), this probe is not ideal for visualizing PKC in intact cells, but would be a valuable fluoroprobe to investigate the kinetic properties of purified PKC. Also, knowledge gained from these studies allows us to predict structures of fluorescent phorbols likely to have less non-specific binding and, consequently, be potentially useful for monitoring PKC in viable cells.

Key words: protein kinase C, flow cytometry, image cytometry, fluorescence anisotropy, fluorescence recovery after photobleaching

The ubiquitous calcium and phospholipid-dependent, diacylglycerol-activated protein kinase, protein kinase C (PKC), has a prominent role in the control of cell proliferation and differentiation and in the transduction of diverse biological signals including certain hormones, growth factors, antibodies, cytokines, and neurotransmitters [1–3]. These substances induce the production of diacylglycerols in their target cells via a number of pathways [4,5] which, in turn, activate PKC [1,3]. The tumor-promoting phorbol esters bind to PKC with high affinity and are potent activators of PKC (for review see reference [6]). Consequently, PKC is considered to be the high affinity cellular receptor that mediates the effects of phorbol esters on cell proliferation [6].

Our aims were to develop fluorescent phorbol ester derivatives to indirectly monitor the subcellular location of PKC. We synthesized phorbol-

Abbreviations used: EBV, Epstein-Barr virus; FRAP, flourescence recovery after photobleaching; [^{3}H]-PDBu, [20(n)-^{3}H]phorbol-12,13-dibutyrate; N-C_{12}-Ac(13), phorbol-13-acetate-12-N-methyl-N-4-(N,N'-di(2-hydroxyethyl)amino)-7-nitrobenz-2-oxa-1,3-diazole aminododecanoate; PBS, phosphate buffered saline; PDBu, phorbol-12,13-dibutyrate; PI, propidium iodide; PKC, protein kinase C; TPA, 12-O-tetradecanoylphorbol-13-acetate.

Received December 10, 1990; accepted March 28, 1991.

Address reprint requests to B.G. Feuerstein or H. A. Pershadsingh, Laboratory for Cell Analysis, Department of Laboratory Medicine, University of California, San Francisco, San Francisco, California 94143-0808.

13-acetate-12-N-methyl-N-4-(N,N'-di(2-hydroxyethyl)amino)-7-nitrobenz-2-oxa-1,3-diazole-aminododecanoate (N-C_{12}-Ac(13)), a fluorescent derivative of 12-O-tetradecanoylphorbol-13-acetate (TPA) and determined its biophysical, biochemical, and biological properties. This compound proved useful for monitoring the subcellular distribution of phorbol ester binding sites in situ in viable cells. The studies also gave clues towards the design of fluorescent phorbol esters capable of specifically labeling PKC intracellularly in situ.

MATERIALS AND METHODS

Reagents

TPA, propidium iodide (PI), and RNAase were purchased from Sigma Chemical Co., St. Louis, MO, and fluorescein isothiocyanate from Molecular Probes Inc., Eugene, OR. All other chemicals were of reagent grade. TPA and its fluorescent derivatives were dissolved in ethanol (stock concentration: 1 mM). The same amount of solvent was applied in control experiments. The final concentration of ethanol never exceeded 0.2%. The monoclonal antibody 2L10 raised against the gp 200/250 membrane antigen complex induced by the Epstein-Barr virus (EBV) [7,8], a kind gift from G.R. Pearson, was labeled with fluorescein isothiocyanate as previously described [9]. [20(n)-^{3}H]phorbol-12,13-dibutyrate ([^{3}H]-PDBu), specific activity 44.8 curies/mmol) was purchased from Amersham.

Synthesis of the Fluorescent Phorbol Ester

12-O-(12-(*N*-methyl-*N*-NBD-amino)) dodecanoyl-phorbol-13,20-diacetate (1). A solution of phorbol-13,20-diacetate (50 mg, 0.11 mmol), 12-*N*-methyl-*N*-NBD-aminododecanoic acid (63 mg, 0.16 mmol), dicyclohexylcarbodiimide (41 mg, 0.2 mmol) and 4-dimethylaminopyridine (4 mg, 0.03 mmol) in 5 ml of dichloromethane was stirred at 0°C for 0.75 h and at room temperature for 24 h. The reaction was filtered and the filtrate partitioned between phosphate buffer (pH 7, 100 mM) and ethyl acetate. The organic layer was separated and dried. Removal of solvent under reduced pressure gave an orange glass, which was chromatographed over silica gel with ethyl acetate-hexanes (2:1) elution to give 99 mg of partially purified material as an orange glass.

12-O-(12-(N-methyl-N-NBD-amino))dodecanoyl-phorbol-13-acetate (N-C_{12}-Ac(13)). A solution of partially purified **1** (99 mg) in 25 ml of methanol and 0.035 ml of perchloric acid was stirred at room temperature for 72 h. The pH was adjusted to 6.5 with 0.5 M sodium methoxide in methanol and the solution concentrated under reduced pressure. The concentrate was partitioned between phosphate buffer (pH 7, 100 mM) and ethyl acetate. The organic layer was separated and dried. Removal of solvent under reduced pressure gave an orange glass which was chromatographed over silica gel with ethyl acetate-hexanes (2:1, then 4:1) elution give 53 mg (62% from phorbol-13,20-diacetate) of N-C_{12}-Ac(13) as an orange glass: TLC (silica gel, ethyl acetate) one fluorescent yellow spot (Rf = 0.6) that chars with chromic acid and heat; ^{1}H NMR ($CdCl_3$, 400 MHz) δ 8.42 (d, 1, J = 9 Hz, Ar), 7.57 (s, 1 H-1), 6.08 (d, 1, J = 9 Hz, Ar), 5.67 (d, 1, J = 4 Hz, H-7), 5.38 (d, 1, J = 10 Hz, H-12), 4.03 (m, 4, 2H-20 and N-CH_2), 3.47 (bs, 3, N-CH_3), 3.24 (bs, 1, H-10), 2.55 (m, 4, 2H-5 and 2H-8), 2.32 (m, 2, -CH_2-CO_2-), 2.09 (s, 3, CH_3C=O), 1.75 (bs, 5, CH_3-19, -CH_2-) 1.62 (m, 3, 1, H-11, -CH_2-), 1.27 (m, 14, 7-CH_2-), 1.20 and 1.23 (2s, 6, CH_3-16 and 17), 1.08 (d, 1, J = 5 Hz, H-14), 0.87 (d, 3, J = 6 Hz, CH_3-18). The structural formulae of TPA and its fluorescent derivative, N-C_{12}-Ac(13), are shown in Figure 1.

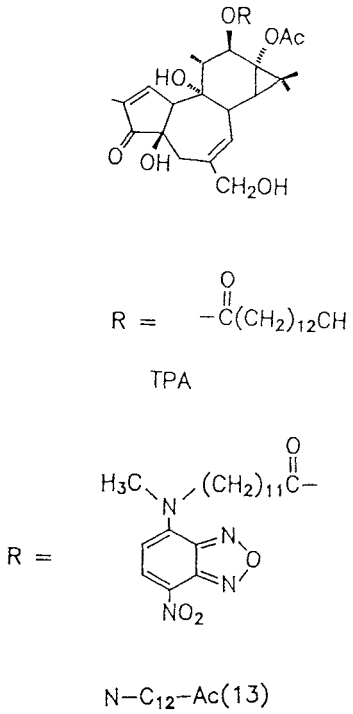

Fig. 1. Structural formulae of TPA and its NBD-labeled fluorescent derivative. The structure of the phorbol skeleton is shown at the top with acetate at carbon-13. The letter N is short for NBD.

Cell Cultures

The P_3HR-1 B lymphocyte cell line is of Burkitt lymphoma origin [10] and can be induced to produce EBV by incubation with TPA [11]. DD cells derived from a human histiocytic tumor line (established by Ferenc Bojan, Department of Hygiene and Public Health, University Medical School, Debrecen, Hungary) can be induced to differentiate into macrophages by treatment with TPA (F. Bojan, personal communication). *Promyelocytic* HL60 human leukemia cells [12] can be induced to differentiate into macrophages by incubation with TPA [13]. All cells were cultured in RPMI-1640 medium supplemented with 10% fetal calf serum. Except where indicated, cells were harvested, washed twice, and resuspended at a concentration of 5×10^5 cells/ml in phosphate buffered saline (PBS) containing: 137 mM NaCl, 2.7 mM KCl, 8.7 mM Na_2HPO_4, 1.45 mM KH_2PO_4, pH 7.4. Unless indicated, all experiments were conducted at 25°C.

Flow Cytometry

Flow cytometric measurements were performed with a Becton-Dickinson FACS III flow cytometer. DD cells stained with PI were illuminated with the argon-ion laser 488 nm excitation line (400 mW output) and fluorescence emission monitored through a 620 nm long-pass dyed glass filter. The fluorescence intensity distribution histograms were transferred to a PDP-11/34 minicomputer and analyzed to quantify the percentage of cells residing in different phases of the cell cycle [14]. The fluorescence of P_3HR-1 cells labeled with N-C_{12}-Ac(13) was analyzed identically, except that a 520 nm long-pass interference filter (Omega Optical, Brattleboro, VT) was used to monitor fluorescence emission. In this case the mean values of the distribution curves were obtained for the first 90% of cells, thus minimizing the effect of the tail of the curves on the calculation.

Steady-State Fluorescence Polarization Measurements

Fluorescence polarization measurements were performed in a Hitachi MPF-4 fluorescence spectrophotometer equipped with polarizers. The polarization of fluorescence was expressed as the fluorescence anisotropy $A = (I_\parallel - I_\perp)/(I_\parallel + 2I_\perp)$, where the $I_\parallel$ and $I_\perp$ are the polarized fluorescence intensities parallel and perpendicular to the direction of the exciting beam, respectively. The total fluorescence: $F = I_\parallel + 2I_\perp$, was also monitored to detect changes in the mean lifetime of the probe's excited state.

Microspectrofluorometric Imaging Analysis

The spatial distribution of N-C_{12}-Ac(13) inside the cell was analyzed with the ACAS 470, an argon-laser interactive fluorescence cytometer [15,16]. P_3HR-1 cells were attached to coverslips by coating them with CELL-TAK (Biopolymers, Farmington, CT), incubated with 100 nM N-C_{12}-Ac(13) for 25 min and mounted on the stage of the inverted microscope. The automated stage moves the sample at 0.25 micron steps in a two-dimensional grid across the objective lens. The fluorescent sample was excited by illuminating it with the 488 nm argon laser line and the emission intensity monitored above 530 nm using a long-pass filter. The emission at each addressed excitation point was monitored by a photomultiplier detector, registered, reconstructed as planar or topographic images in two dimensions, and displayed on a color monitor. The cellular fluorescence image is presented using a pseudo-color scale of fluorescence intensity.

Inhibition of [^{3}H]-PDBu Binding With N-C_{12}-Ac(13)

Freshly isolated Sprague-Dawley female rat brain was homogenized for 20 min in 30 ml of buffer (20 mM Tris-HCl, pH 7.5, 0.25 M sucrose, 10 mM EGTA, 2 mM EDTA, and 1 mM phenylmethylsulfonyl fluoride) with a rotating pestle and Dounce homogenizer in ice. The homogenate was centrifuged at 25,000*g* for 1 h. The supernatant cytosol was kept frozen and pellet discarded. Binding was initiated by adding 25 μl of cytosol to a 75 μl of reaction mixture containing 30 mM Tris buffer (pH 7.5), 6 mM Mg acetate, 0.5 mg/ml bovine serum albumin, 20 μg/ml phosphatidylserine (suspended in buffer by sonication for 5 min), 0.5 mM calcium chloride, and 50 nM [^{3}H]-PDBu. Non-specific binding was determined in the presence of 100 μM unlabeled phorbol-12,13-dibutyrate (PDBu). The reaction mixture was mixed and incubated at room temperature for 15 min. Samples of 75 μl were spotted on Whatman DE81 DEAE filter discs. The discs were allowed to stand for 5 min and reaction terminated by dropping into ice-cold 20 mM Tris buffer (pH 7.5). The discs were washed four times with the same buffer. The

samples were counted in 5 ml of scintillation liquid.

Fluorescence Photobleaching and Recovery

The mobility of N-C_{12}-Ac(13) bound to the cell was determined with the ACAS 470 using its capability to analyze fluorescence redistribution after photobleaching (FRAP) [15]. A spot on the cell 1 micron in diameter is bleached by a pulse of the focused laser beam for 50 milliseconds. The laser beam is then attenuated and used to monitor the recovery of fluorescence within the bleached region. This was performed at different locations within cells for comparative purposes. The data were analyzed for diffusion coefficient and percent of recovery obtained, as previously described [17,18].

Induction of EBV Expression in P_3HR-1 Cells

P_3HR-1 cells were grown to a density of at least 2×10^6 cells/ml, diluted to 5×10^5 cells/ml, and the concentration of fetal calf serum in the medium decreased to 5%. Cells were incubated with unlabeled TPA or N-C_{12}-Ac(13), (final concentrations: 65 and 51 nM, respectively) for 48 h at 37°C, harvested, washed twice, and resuspended in PBS at 2×10^7 cell/ml. An aliquot (100 μl) of the cell suspension was labeled with fluorescein-conjugated 2L10 monoclonal antibody (0.1 mg/ml) by incubation for 1 h at 0°C, washed twice with PBS, fixed and stored in PBS containing 1% formaldehyde. This antibody recognizes cells induced to express glycoprotein gp 200/250 EBV viral antigen complex. The percentage of positive cells (i.e., cells expressing the viral glycoprotein) was determined manually using an Olympus BHT-2 fluorescence microscope.

Induction of Changes in Cell Cycle Kinetics

Cell cycle analysis of DD cells was performed as previously described [19]. Briefly, DD cells were treated with TPA or N-C_{12}-Ac(13) (final concentrations: 65 nM and 51 nM, respectively) for 24 h at 37°C. Control samples were treated identically with the ethanol solvent. Suspensions of DD cells in PBS were fixed by exposure to gradually increasing concentrations of ethanol (−20°C) up to 70% v/v over a 30-min interval in an ice bath where they were stored prior to use. DNA content was analyzed in cells treated with RNAase (0.1 mg/ml) for 1 h at 37°C and subsequently stained with 30 μg/ml PI for 30 min [20].

Induction of Differentiation of HL60 Cells

HL60 cells were seeded into Falcon plastic flasks at a concentration of 3×10^5 cell/ml and TPA or N-C_{12}-Ac(13) (final concentrations: 65 nM and 51 nM, respectively) were added. After incubation for 48 h at 37°C, differentiation of the premature promyelocytic HL60 cells into mature macrophages was qualitatively assessed as their ability to adhere to the surface of the culture flask, as determined by phase contrast microscopy. Adherence indicated differentiation.

RESULTS

Fluorescence Characteristics of N-C_{12}-Ac(13) Bound to P_3HR-1 Cells

The uptake of N-C_{12}-Ac(13) by P_3HR-1 cells was monitored both by flow cytometry and spectrofluorometry. Uptake kinetics in fixed and live cells were nearly the same. N-C_{12}-Ac(13) is virtually nonfluorescent in aqueous solution alone, being one-fourth the intensity of the autofluorescence of a cell suspension. As shown in Figure 2, addition of cells to PBS containing 100 nM N-C_{12}-Ac(13) greatly enhanced the fluorescence intensity of the suspension (20-fold increase). Steady-state fluorescence was achieved within 20–25 min. Because the fluorescence of N-C_{12}-Ac(13) in the extracellular medium was negligible compared with that bound to cells, stained cell suspensions were routinely analyzed without washing. At the lower limit, we could detect 20 nM of the compound in our cells. The fluorescence spectra of N-C_{12}-Ac(13) taken up by cells are

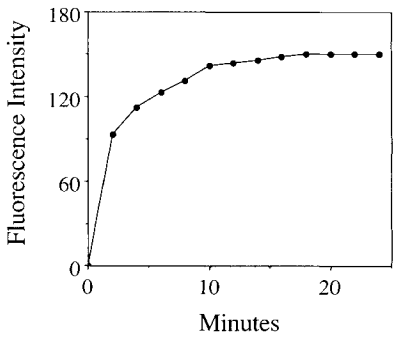

Fig. 2. Time-dependent uptake of N-C_{12}-Ac(13) by P_3HR-1 cells. N-C_{12}-Ac(13) (100 nM) was added to P_3HR-1 cells (5×10^5 cell/ml) suspended in a cuvette containing 3 ml PBS and incubated at 25°C (all experiments were conducted at this temperature unless indicated otherwise). Fluorescence intensity (excitation: 490 nm; emission: 520 nm; slit-width: 5 nm) was recorded as a function of time.

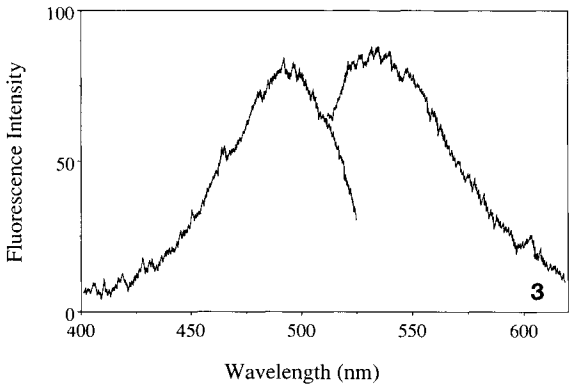

Fig. 3. Excitation (left curve) and emission (right curve) fluorescence spectra of N-C_{12}-Ac(13). The excitation (emission: 520 nm; 5 nm slit-width) and emission (excitation: 490 nm; 5 nm slit-width) spectra of P_3HR-1 cells suspended in PBS (5×10^5 cell/ml) labeled with 100 nM N-C_{12}-Ac(13) for 25 min. Other experimental details are the same as described for Figure 2.

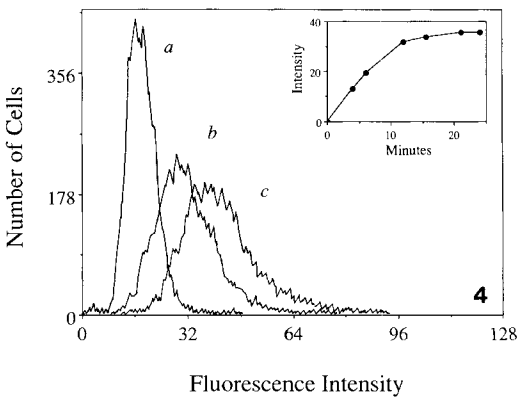

Fig. 4. Flow cytometric measurements of N-C_{12}-Ac(13) fluorescence. Frequency distribution histograms of fluorescence intensities of P_3HR-1 cells incubated with 100 nM N-C_{12}-Ac(13) recorded at 5 (**a**), 15 (**b**), and 25 (**c**) min. **Inset:** Mean values of the distribution curves plotted as a function of time.

shown in Figure 3 and were almost identical to that of N-C_{12}-Ac(13) dissolved in toluene. The spectra show that in contrast to the commercially available fluorescent dansyl derivatives of TPA [21] which can be excited only at short wavelengths in the ultraviolet region of the spectrum, N-C_{12}-Ac(13) can be strongly excited at 488 nm in the visible spectrum.

Fluorescence intensity distribution curves of cells incubated with N-C_{12}-Ac(13) for 5, 15, and 25 min, determined by flow cytometry, are shown in Figure 4. The steady-state level of fluorescence intensity was reached after 25 min (shown in the inset), when mean values of distribution histograms are plotted as a function of time. These findings are similar to those obtained by spectrofluorometric analysis (Fig. 2).

The fluorescence intensity of N-C_{12}-Ac(13) labeled cells was one-third that of a toluene solution containing the same concentration of N-C_{12}-Ac(13). The fluorescence anisotropy values obtained for N-C_{12}-Ac(13) in solution in toluene and bound to P_3HR-1 cells, were 0.005 ± 0.002 and 0.226 ± 0.008, respectively. The high fluorescence anisotropy value obtained with the cells could be caused by a decrease in the fluorescence lifetime (average excited state lifetime) and/or by a decrease in the rotational relaxation time (indicative of a decrease in rotational diffusion) of the fluorophore. The fluorescence intensity of N-C_{12}-Ac(13) dissolved in tetrahydrofuran was the same as that of cells labeled with same amount of N-C_{12}-Ac(13), suggesting that the average fluorescence lifetime of the probe is similar in both cases because fluorescence intensity is proportional to the excited state lifetime. The fluorescence anisotropy value of N-C_{12}-Ac(13) in tetrahydrofurane was 0.040 ± 0.005, showing that the decrease in fluorescence lifetime caused only a slight increase in fluorescence anisotropy as compared with that measured in toluene. These observations suggest that the high fluorescence anisotropy value of N-C_{12}-Ac(13) in cells is due mainly to a decrease in rotational diffusion of the N-C_{12}-Ac(13) in the cellular environment.

Subcellular Distribution of N-C_{12}-Ac(13) in P_3HR-1 Cells

P_3HR-1 cells were labeled with 100 nM N-C_{12}-Ac(13) and the cells analyzed on the ACAS 470 laser cytometer. Maps showing the distribution of fluorescence within P_3HR-1 cells were generated using a pseudo-color scale of fluorescence intensity (Fig. 5A,B). The distribution of N-C_{12}-Ac(13) fluorescence in the cytoplasm was uneven with bright regions arranged in a crescentic partially perinuclear pattern. The cells showed minimal labeling within the nuclear region. Although not shown, the nucleus is prominent and can easily be identified under bright-field microscopy. An identical pattern was seen in cells fixed with paraformaldehyde and washed prior to staining with N-C_{12}-Ac(13) (data not shown). Fixation permeabilizes the cells and washing would remove soluble cytoplasmic contents. Therefore, these findings suggest that the

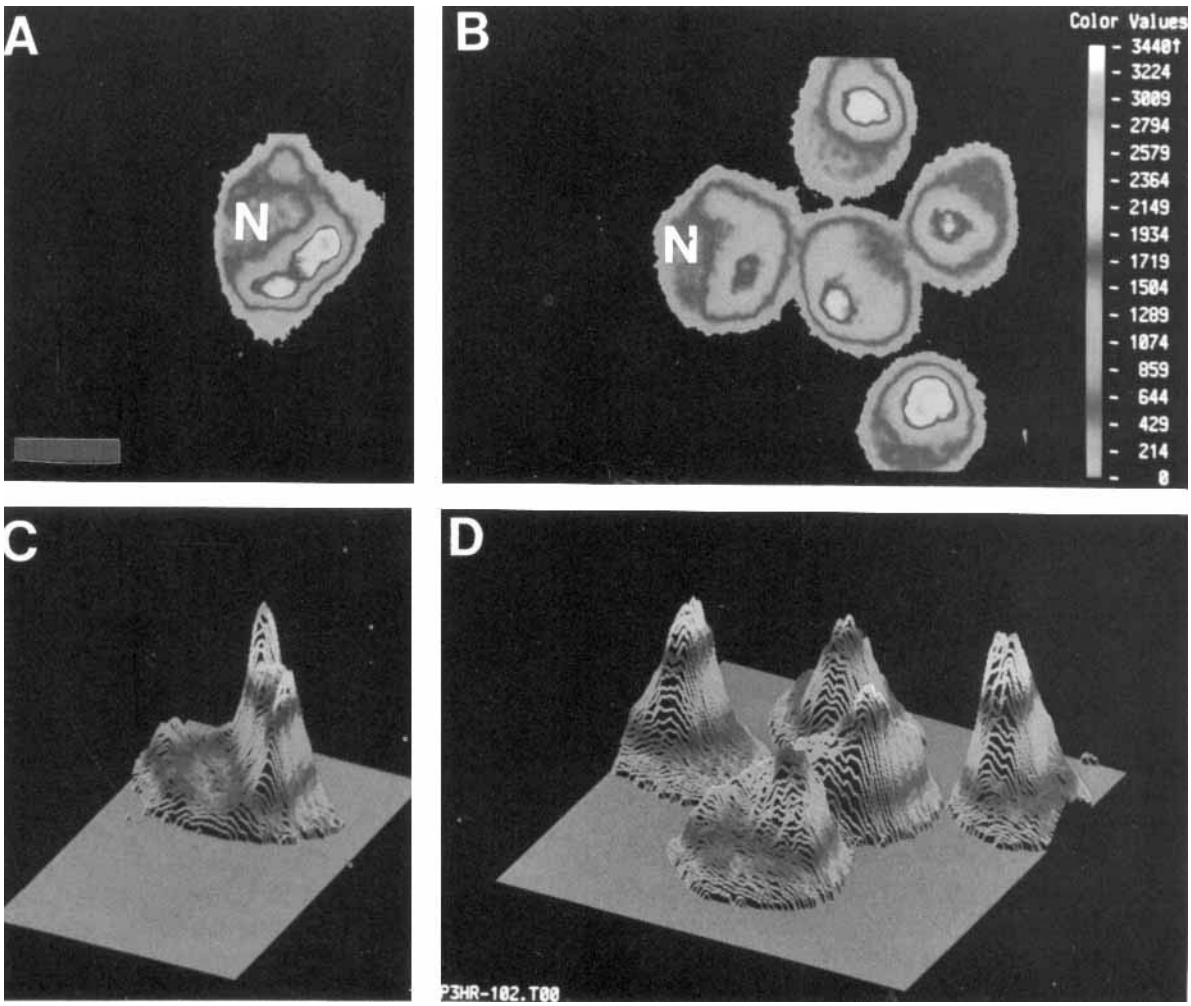

Fig. 5. Subcellular distribution of N-C_{12}-Ac(13) fluorescence. Pseudo-color digitized computer images (shown above in black and white) of fluorescence intensity of P_3HR-1 cells labeled with 100 nM N-C_{12}-Ac(13) **(panels A and B).** The images in panels A and B are presented topographically as a three-dimensional plots **(panels C and D),** with the fluorescence intensity on the Z axis. The topographic images were rotated by 90°C. Where indicated, the letter "N" designate the nuclear regions. The bar represents 10 microns. Color values are shown with their numerical equivalency on an arbitrary scale for fluorescence intensity. (See cover for color illustration.)

probe binds to membranous and other non-soluble structures in the cell. The data can be better visualized when presented topographically with fluorescence intensity on the Z-axis, where the low level of nuclear fluorescence appears as a "craters" (Fig. 5C,D). The depth-of-focus of the laser beam is approximately 7 to 8 microns, and although variations in cell thickness contribute to variations in the intensity of the fluorescence image, the topographical distribution of cell-associated fluorescence differs dramatically from that expected from a uniformly labeled cell with the typical spherical geometry of P_3HR-1 cells (Fig. 5C,D).

Determination of N-C_{12}-Ac(13) Diffusion in P_3HR-1 Cells

Diffusion of N-C_{12}-Ac(13) at various subcellular locations was investigated using the FRAP technique (see Materials and Methods). The rate of lateral diffusion of N-C_{12}-Ac(13) was determined at different locations within P_3HR-1 cells. This was done by locating the site for bleaching at different regions within the cell: the bright cytoplasmic, the dim nuclear, or the peripheral cytoplasmic (plasma membrane) regions. No significant difference was detected in the rate of diffusion measured at these different regions

within the cell. The mean recovery of fluorescence was 65 ± 11% (range: 50 to 80%; n = 8) and the lateral diffusion coefficient was $(2.0 \pm 0.3) \times 10^{-8}$ cm^2 sec^{-1}.

Demonstration of Specific Binding of N-C_{12}-Ac(13)

Binding properties of N-C_{12}-Ac(13) was studied in intact cells and in partially purified rat brain cytosol samples.

Binding of N-C_{12}-Ac(13) to P_3HR-1 cells. The specificity of binding of N-C_{12}-Ac(13) to P_3HR-1 cells was evaluated by means of competition experiments with unlabeled TPA. TPA caused a decrease in total cellular fluorescence of N-C_{12}-Ac(13)-labeled cells regardless of the order of addition of probe or unlabeled compound. Figure 6 shows the effect of various concentrations of TPA on the fluorescence intensity of cells stained with 100 nM N-C_{12}-Ac(13). There was a progressive reduction in cell-associated fluorescence with increasing concentrations of TPA reflecting competitive displacement of N-C_{12}-Ac(13) by unlabeled TPA. The reduction in the fluorescence intensity of cells exposed to extremely high concentrations of TPA was not greater than 50% of labeled cells without TPA, indicating a significant amount of nonspecific binding of the probe, most likely to hydrophobic lipid regions.

Binding of N-C_{12}-Ac(13) to rat brain cytosol. In order to ascertain the binding specificity of N-C_{12}-Ac(13) fluoroprobe, we tested its ability to compete with [^{3}H]-PDBu for the phorbol ester binding site of PKC. Since it has been well

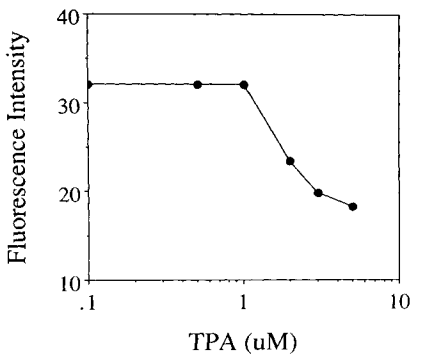

Fig. 6. Competition between N-C_{12}-Ac(13) and unlabeled TPA. P_3HR-1 cells (5×10^5 cell/ml) were incubated with 100 nM *N-C_{12}-Ac(13) in the presence* of TPA at various concentrations for 25 min and fluorescence measured by flow cytometry. The mean values of fluorescence intensity distribution curves were plotted as a function of TPA concentration.

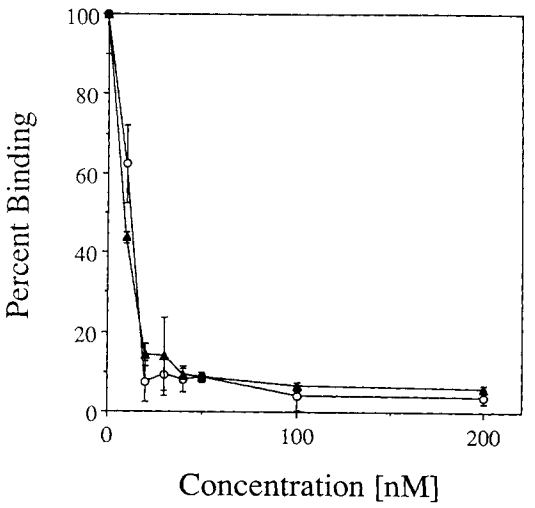

Fig. 7. Competitive displacement of [^{3}H]-PDBu by TPA and N-C_{12}-Ac(13). [^{3}H]-PDBu bound to partially purified rat brain PKC was displaced by TPA (**open circles**) and N-C_{12}-Ac(13) (**full triangles**) at room temperature. Percent of [^{3}H]-PDBu binding is plotted versus concentration of N-C_{12}-Ac(13) or TPA. Binding studies were performed as described in Materials and Methods. Bars represent one standard deviation.

demonstrated that the presence of inhibitor(s) of PKC activity does not interfere with [^{3}H]-PDBu binding measurements [6], the binding studies were performed with crude rat brain cytosol. Figure 7 shows that N-C_{12}-Ac(13) competed effectively with [^{3}H]-PDBu for the phorbol binding site with an approximate K_d value of 11 nM. This compared with the K_d value of 12 nM for the displacement of [^{3}H]-PDBu by TPA. The results indicate that N-C_{12}-Ac(13) fluoroprobe does bind PKC with high affinity.

Biological Effects of N-C_{12}-Ac(13)

Three different systems were used to compare the bioactivity of TPA with its NBD-conjugated derivative.

Phorbol ester-induced changes in DD cell cycle distribution. The DNA content was quantified by staining DD cells with PI, a dye that specifically intercalates within double-stranded DNA [19,20]. Figure 8 shows the distribution histograms of PI fluorescence in DD cell populations at various stages of the cell cycle. Distribution histograms of control cell suspensions and those treated with TPA (65 nM) or N-C_{12}-Ac(13) (51 nM) are shown (Fig. 8A–C, respectively). Quantification of various regions of the cell cycle derived from the distribution histograms (Fig. 8) are shown in Table I and are expressed as percentages of the total integrated

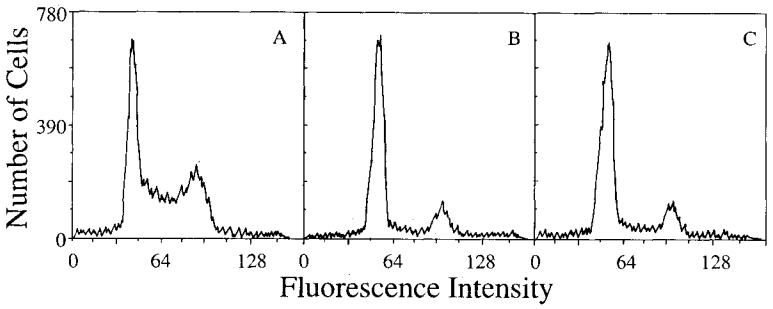

Fig. 8. Effects of TPA and N-C_{12}-Ac(13) on the mitotic cycle. Fluorescence intensity distribution curves of DD cells stained with PI (30 μg/ml), a fluorescent DNA stain, after RNAase treatment. Cells were treated for 24 h at 37°C with the phorbol ester solvent, **(A)** 0.01% ethanol; **(B)** 65 nM TPA; **(C)** or 51 nM N-C_{12}-Ac(13).

area under each histogram (error range: ±2 to 3%). Control cells show a characteristic distribution, with the majority of cells residing in the G1 phase and the remainder distributed roughly equally between the S phase and the G2 plus mitotic phases. Incubation of cells with 65 nM TPA (Fig. 8B) or 51 nM N-C_{12}-Ac(13) for 24 h caused changes in cell cycle distribution characteristic of a block in G1 to S transition, with more cells present in the G1 phase and less in the S phase (Table I). These observations indicate that, biologically, N-C_{12}-Ac(13) has similar effects as TPA on cell cycle distribution.

Phorbol ester-induced differentiation of HL60 cells. Undifferentiated HL60 promyelocytic cells grow in suspension and are ordinarily non-adherent. However, when incubated with 65 nM TPA for 48 h, they differentiate into mature macrophages and the majority (approximately 80%) adhere to the surface of the culture flask [13]. Trypsin treatment was required for removal of the adherent cells. At 51 nM, N-C_{12}-Ac(13) was as effective as 65 nM TPA in inducing differentiation of HL60 cells into macrophages (Table I).

TABLE I. Biological Activity of the TPA and Its Fluorescent Derivative N-C_{12}-Ac(13)*

Treatment	P_3HR1 Cells % of cells with viral antigen	HL60 Cells Increase in cell adherence	DD Cells Changes in cell cycle
Solvent	2	negative	G1: 41% S: 33% G2 + M: 26%
TPA (65 nM)	28	positive	G1: 62% S: 17% G2 + M: 21%
N-C_{12}-Ac(13) (51 nM)	27	positive	G1: 62% S: 18% G2 + M: 20%

*The biological effects of the phorbol esters in three different bioassay systems were evaluated as described in Materials and Methods. Cells were treated with 65 nM TPA or 51 nM N-C_{12}-Ac(13) and the results were compared with the effect of an equivalent concentration of solvent (0.01% ethanol). Error range: ± 2 to 3%.

Phorbol ester-induced expression of viral antigen in P_3HR-1 cells. In the P_3HR-1 lymphoma line, the EBV viral cycle is spontaneously induced in 2–3% of the cells and membrane antigen complexes are expressed on the cell surface. The gp 200/250 glycoprotein membrane antigen complex was detected by monitoring the fluorescence of fluorescein-conjugated 2L10 monoclonal antibody. The percentage of positive cells (i.e., those expressing the gp 200/250 glycoprotein) increased significantly from 2–3% to 29 ± 4% and 27 ± 3% when treated with TPA or N-C_{12}-Ac(13), respectively (Table I). These data also indicate that N-C_{12}-Ac(13) possesses biological activity equivalent to that of unlabeled TPA.

DISCUSSION

A wide constellation of dissimilar physiologic ligands control the active state of cells by inducing them to produce diacylglycerols, a class of second messengers that regulate diverse cellular functions through complex interactions with PKC [1–3,22,23]. Tumor-promoting phorbol esters bind to purified PKC with high affinity and activate the enzyme by substituting for diacylglycerol [6]. Both the binding of tumor-promoting phorbol esters to PKC and the enzyme activity of PKC require the presence of calcium and phospholipid, and the tissue distribution of PKC follows that for phorbol ester binding. More-

over, the demonstration that phorbol ester-binding activity and PKC enzyme activity co-purify [24] suggests that the major high affinity phorbol ester-binding protein is PKC. Therefore, PKC is thought to be the high affinity cellular receptor that mediates the effects of phorbol esters on cell proliferation [2,5,25]. Consequently, calcium and phospholipid-dependent phorbol-ester high affinity binding capacity has been used to quantify PKC activity, regardless of the presence of endogenous inhibitors or activators [6].

PKC is not a single enzyme, but a family of isoforms that vary in their kinetic requirements for calcium, diacylglycerol, and phospholipid [26,27]. Also, there are distinct patterns of isoenzyme expression not only among different tissues, but also in the distribution of these isotypes within cells of particular tissues and organs [27,28]. PKC has the unique ability to behave as a membrane-bound and a cytoplasmic enzyme. It is not normally active in the cytosol, but can be rendered so by specific protease-mediated cleavage [27–29]. Therefore, spatial disposition and proteolysis provide additional dimensions of organization whereby hormonal signals mediated by PKC may be transmitted to its subcellular target substrates.

Our objective was to invent a method to monitor PKC in situ in living cells. To accomplish this we synthesized the tetradecanoyl phorbol derivative N-C_{12}-Ac(13) and determined whether or not it could function as an indirect fluorescent probe of PKC. The excitation spectrum of N-C_{12}-Ac(13) bound to cells has a maximum at 510 nm with a prominent shoulder at 490 nm, allowing for convenient use of the 488 nm argon laser excitation line, thus extending its applicability to argon ion laser-based flow and imaging cytometers. N-C_{12}-Ac(13) is strongly quenched in aqueous solution, so that the contribution of dye fluorescence associated in the extracellular medium was negligible. This was particularly convenient in studies using spectrofluorometry, flow, and imaging cytometry, as removal of extracellular dye was unnecessary. Therefore, cells were routinely analyzed under dynamic equilibrium conditions. Because the dye is present in the bathing medium during analysis, it may redistribute with more probe entering and/or leaving the cells. The probe fluoresces strongly when bound to cells, giving a signal 20-fold above autofluorescence within 25 to 30 min at 25°C when incubated with 100 nM dye, at which time the probe is maximally accumulated and net flux approaches zero.

Several lines of evidence suggest that N-C_{12}-Ac(13) might be useful as an indirect probe of PKC. The fluorescence intensity of N-C_{12}-Ac(13) decreases in a dose-dependent manner by addition of unlabeled TPA and can be explained as the relocation of the fluoroprobe to a more polar molecular environment where its quantum yield is diminished. Presumably, N-C_{12}-Ac(13) molecules bound to PKC are competitively displaced by TPA, indicating specific binding of N-C_{12}-Ac(13). Competitive displacement studies are best done under conditions in which trace (subnanomolar) amounts of the probe are used. Because of limitations due to quantum efficiency of N-C_{12}-Ac(13), we used 100 nM, clearly not a subnanomolar amount. It is therefore not surprising that displacement is not seen until the concentration of unlabeled TPA approaches 1 μM. Because of the lipophilicity bestowed by the dodecanoyl fatty acyl chain, a significant amount of the fluoroprobe likely binds non-specifically to lipids, resulting in incomplete displacement by unlabeled TPA. A further limitation placed on displacement studies done under these conditions is related to the fact that because of its hydrophobic nature, TPA has an upper limit of solubility in aqueous buffers of approximately 3 μM, above which it forms micelles. Nevertheless, our studies on the displacement of [^{3}H]-PDBu with N-C_{12}-Ac(13) on rat brain cytosol revealed a single high affinity binding site with a K_d of 11 nM, which is similar to that obtained for the binding of TPA to purified brain PKC [30].

Fluorescence polarization studies indicate that N-C_{12}-Ac(13) does not rotate freely in the cell as a small molecule, but probably binds to the hydrophobic region of PKC, whether located in the cytoplasm or associated with membranous structures in the cell. The diffusion coefficient value of N-C_{12}-Ac(13) determined by FRAP is similar to that determined for diffusion of lipids or proteins loosely associated to the membrane [31], also suggesting that the probe is bound to protein or embedded in the membranes of the cell. Incomplete recovery of fluorescence (65 vs. 100%), which usually occurs in case of binding to proteins, indicates that the remaining 35% of the fluorescent probe is sequestered within non-diffusible compartment(s) inside the cell [32].

Importantly, in three different preparations, rat Purkinje cells [3], GH_4C_1 anterior pituitary

cells [33], and 3T3-L1 fibroblasts [34], immunofluorescent labeling of PKC shows a distribution similar to that obtained with N-C_{12}-Ac(13). Also, the subcellular distribution of N-C_{12}-Ac(13) is similar to that obtained with another fluorescent phorbol ester, dansyl-12-O-tetradecanoyl phorbol acetate [21]. At present the subcellular distribution of PKC is usually assessed by means of [^{3}H]-phorbol-12,13-dibutyrate or indirect immunofluorescence staining with specific anti-PKC antibodies. The former is cumbersome and time-consuming, involving fractionation of cells and quantifying the number of high affinity [^{3}H]-phorbol-12,13-dibutyrate binding sites in the subcellular fractions based on protein concentration [35]. The latter requires fixation of cells that involve washing procedures resulting in removal of soluble PKC [33,34] and is dependent on the specificity of the primary antibody. In both cases, it is not possible to visualize the subcellular location of PKC in viable cells. Use of fluorescent phorbol esters offers the potential advantage of monitoring PKC in viable cells in situ. By using the ACAS 470 and a phorbol fluoroprobe with high specificity, one can monitor the relocation of N-C_{12}-Ac(13) subcellularly subsequent to activation by physiological and pharmacological stimuli.

Biological activity of N-C_{12}-Ac(13) was assessed using three different bioassays. Like TPA, an equivalent concentration of N-C_{12}-Ac(13) induced expression of EBV antigen on the surface of P_3HR-1 cells, promoted differentiation of HL60 promyelocytic cells, and caused predictable changes in the mitotic cycle of histiocytic DD cells. If one accepts that the biological effects of TPA are due to its binding to cellular PKC, then one must also conclude that N-C_{12}-Ac(13) also binds to PKC under the same conditions.

Therefore, this newly developed, biologically active fluorescent analog of TPA can be used to monitor the location of phorbol ester binding sites in living cells. By imaging the probe subcellularly one might obtain spatial information on agonist-induced translocation of phorbol ester subcellularly in situ. However, because of its significant non-specific binding, N-C_{12}-Ac(13) may not be an ideal candidate for monitoring PKC in situ. Nevertheless, it may be used to optically probe the enzymatic properties of PKC and the enzyme's interactions with natural cofactors in cell-free systems where nonspecific binding is not an impediment. It is possible that N-C_{12}-Ac(13) and similar phorbol fluorochromes might be useful tools for probing enzymatic differences between various PKC isotypes. Fluorescent derivatives of phorbol diesters that have lower non-specific binding to lipid hydrophobic domains, diminished ability to activate the enzyme, and bind to PKC specifically with high affinity will be better candidates for probing the subcellular location of PKC in situ in viable cells. Altering the hydrophobicity of the phorbol ester by altering the chain length of the aliphatic carbon chain and blocking the kinase activity of PKC through use of known inhibitors are possible solutions to these problems.

ACKNOWLEDGMENTS

Supported by a research grant from the Max and Victoria Dreyfus Foundation (H.A.P.), Hungarian Academy of Sciences grant OTKA 112 (M.B., J.S., S.D.), and NIH grants 1R43 GM37347 (R.P.H.) and CA 41757 (B.G.F.). H.A.P. is the recipient of an American Diabetes Association Research and Development Award and a grant from the Max and Victoria Dreyfus Foundation. The authors wish to thank Barbara Laughter (Meridian Instruments, Inc.) for analyzing the imaging data and Dr. R.L. Bernstein for helpful discussions.

REFERENCES

1. Berridge MJ: Biochem J 220:345–360, 1984.
2. Nishizuka Y: Nature 308:693–698, 1984.
3. Nishizuka Y: Science 233:305–312, 1986.
4. Niedel JE, Kuhn LJ, Vanderbark GR: Proc Natl Acad Sci USA 80:36–40, 1983.
5. Niedel JE, Blackshear PJ: In Putney JE (ed): "Phosphoinositides and Receptor Mechanisms." New York: Alan R. Liss, Inc., pp 47–88, 1986.
6. Leach KL, Blumberg PM: In Michell RH, Drummond AH, Downes CP (eds): "Inositol Lipids in Cell Signalling." New York: Academic Press, 179–205, 1989.
7. Qualtiere LF, Chase R, Pearson GR: J Immunol 129: 814–818, 1982.
8. Qualtiere LF, Chase R, Vroman B, Pearson GR: Proc Natl Acad Sci USA 79:616–620, 1982.
9. DePetris S: In Korn ED (ed): "Methods in Membrane Biology." New York: Plenum Press, vol 9, pp 1–201, 1978.
10. Hinuma Y, Konn M, Yamaguchi J, Wudarski DJ, Blakeslee JR Jr., Grace JT, Jr.: J Virol 1:1045–1051, 1967.
11. Zur Hausen H, Bornkamm GW, Schmidt R, Hecker E: Proc Natl Acad Sci USA 76:782–785, 1979.
12. Collins SJ, Gallo RC, Gallagher RE: Nature 270:347–349, 1977.
13. Rovera G, O'Brian TG, Diamond L: Science 204:868–870, 1979.
14. Dean PN: In Van Dilla MA, Dean PN, Laerum OD, Melamed MR (eds): "Flow Cytometry: Instrumentation

and Data Analysis." New York: Academic Press, pp 195–221, 1985.
15. Schindler M, Trosko JE, Wade MH: Methods Enzymol 141:439–447, 1987.
16. Jiang L-W, Schindler M: J Cell Biol 106:13–19, 1988.
17. Koppel DE: Biophys J 28:281–292, 1979.
18. Koppel DE, Sheetz MP, Schindler M: Biophys J 30:187–192, 1980.
19. Crissman HA, Mullaney PF, Steinkamp JA: In Prescott DM, (ed): "Methods in Cell Biology." New York: Academic Press, vol. 9, pp 179–246, 1975.
20. Steinkamp JA, Crissman HA: J Histochem Cytochem 22:616–621, 1974.
21. Liskamp RMJ, Brothman AR, Arcoleo JP, Miller OJ, Weinstein IB: Biochem Biophys Res Commun 131:920–927, 1985.
22. Michell RH: In Putney JE (ed) "Phosphoinositides and Receptor Mechanisms." New York: Alan R. Liss, Inc., pp 1–24, 1986.
23. Standaert ML, Pollet RJ: FASEB J 2:2453–2461, 1988.
24. Ashendel CL, Boutwell RK: Biochem Biophys Res Commun 99:543–549, 1981.
25. Castagna M, Pavoine C, Bazgar S, Couturier A, Chevalier M, Fiszman M: In Dumont JE, Hamprecht B, Nunez J (eds): "Hormones and Cell Regulation." New York: Elsevier, vol. 9, pp 185–206, 1985.
26. Coussens L, Parker PJ, Rhee L, Yang-Feng TL, Chen E, Waterfield MD, Francke U, Ullrich A: Science 233:859–866, 1986.
27. Nishizuka Y: Nature 334:661–665, 1988.
28. Girard PR, Mazzei GJ, Kuno JF: J Biol Chem 261:370–375, 1986.
29. Kishimoto A, Mikawa K, Yasuda I, Tanaka S, Tominaga M, Kuroda T, Nishizuka Y: J Biol Chem 264:4088–4092, 1989.
30. Kikkawa U, Takai Y, Tanaka Y, Miyake R, Nishizuka Y: J Biol Chem 258:11442–11445, 1983.
31. Wey C-L, Cone RA: Biophys J 33:225–232, 1981.
32. Wier ML, Edidin M: J Cell Biol 103:215–222, 1986.
33. Leach KL, Powers EA, McGuire JC, Dong L, Kiley SC, Jaken S: J Biol Chem 263:13223–13230, 1988.
34. Halsey DL, Girard PR, Kuo JF, Blackshear PJ: J Biol Chem 262:2234–2243, 1987.
35. Pershadsingh HA, Shade DL, McDonald JM: Biochem Biophys Res Commun 145:1384–1389, 1987.